MICROSTRUCTURE AND STRENGTH OF METALS PROCESSED BY SEVERE PLASTIC DEFORMATION

Jenő Gubicza[1,*], Nguyen Quang Chinh[1], Terence G. Langdon[2] and Tamás Ungár[1]

[1]Institute of Physics, Eötvös University, Budapest, P.O.Box 32, H-1518, Hungary

[2]Departments of Aerospace & Mechanical Engineering and Materials Science,

University of Southern California, Los Angeles, CA 90089-1453, USA

Abstract

The microstructure of f.c.c. metals (Al, Cu, Ni) and alloys (Al-Mg) processed by severe plastic deformation (SPD) methods is studied by X-ray diffraction line profile analysis. It is shown that the crystallite size and the dislocation density saturate with increasing strain. Furthermore, the Mg addition promotes efficiently a reduction of the crystallite size and an increase of the dislocation density in Al during the SPD process. The yield strength correlates well with that calculated from the dislocation density using the Taylor equation, thereby indicating that the main strengthening mechanism in both pure metals and alloys is the interaction between dislocations.

Keywords: severe plastic deformation, face-centered cubic metals, X-ray diffraction line profile analysis, dislocation density, strength

Introduction

Severe plastic deformation (SPD) is an effective tool for producing bulk ultrafine-grained metals. The most common SPD methods are equal-channel angular pressing (ECAP) and high pressure torsion (HPT) [1,2]. The ultrafine-grained materials formed by SPD procedures have a very high strength owing to their small grain size and high dislocation density. To understand the mechanical behavior of materials produced by ECAP, it is necessary to characterize their microstructures.

It is well known that the crystallite size and the lattice strain in ultrafine-grained materials can be determined by X-ray line profile analysis [3,4]. In SPD-processed materials where the lattice distortions are primarily caused by dislocations, the characteristic parameters of the dislocation structure can be obtained by an evaluation of the strain broadening of X-ray line profiles [3,4].

In this paper, the evolution of ultrafine-grained microstructure in Al and Al-Mg alloys during ECAP is studied. The effect of Mg addition on the microstructure and on the yield strength is investigated. Furthermore, a correlation is demonstrated between the yield strength (mechanical properties) and the dislocation density (microstructure) of different SPD-processed ultrafine-grained f.c.c. metals including pure Al, Cu and Ni as well as Al-Mg alloys.

---

* Corresponding author. gubicza@ludens.elte.hu

Experimental Material and Procedures

To study the effect of alloying on the microstructure developed during SPD in Al, experiments were conducted on high-purity (4N) Al, Al − 1 wt.% Mg (Al1Mg) and Al − 3 wt.% Mg (Al3Mg) alloys. Before the process, the Al was annealed for 30 min at 400 $^{\circ}$C and the alloys for 1 h at 500 $^{\circ}$C to obtain a defined initial state with grain size of ~200 μm. Cylindrical billets were machined having 10 mm in diameter and ~60 mm length [5,6]. The specimens were processed at room temperature by ECAP up to 8 passes using a 90° die following route B_C. Route B_C means that the billet was rotated around its longitudinal axis in the same direction after each pass by an angle of 90° [7]. It can be shown that an imposed strain of ~1 is introduced on each passage of the sample through the ECAP die [8]. The yield strength of the specimens processed by ECAP was measured at room temperature by compression test using an MTS machine operating with constant grip velocity giving an initial strain rate of 10^{-3} s^{-1}. The compression axis was parallel to the output channel axis of the last ECAP pass. To study the development of the microstructure as a function of strain, annealed samples were also deformed by compression up to a strain of 0.2 at room temperature [6]. The specimens machined for compression tests were in the form of cylinders 5 mm in diameter and 7 mm high.

The microstructure of the deformed specimens was investigated by X-ray diffraction line profile analysis. The X-ray diffraction profiles were measured on the cross-section perpendicular to the axis of compression (for the compressed specimens) or to the output channel of the last ECAP pass. The X-ray diffraction experiments were performed by a special high-resolution diffractometer (Nonius FR591). The instrumental broadening ($\Delta2\Theta=0.006°$) was negligible compared to the measured line broadening ($\Delta2\Theta=0.1$-$0.3°$) therefore instrumental correction was not performed. The diffractometer was operated at 40 kV and 70 mA using a rotating Cu anode (CuKα_1 radiation: =0.15406 nm). The line profiles were evaluated by the Multiple Whole Profile (MWP) fitting procedure described in detail elsewhere [9]. In this method, the Fourier coefficients of the experimental profiles are fitted by theoretical functions calculated on the basis of a model of microstructure in which the size of spherical crystallites has a log-normal distribution and the lattice strains are caused by dislocations. From the fitting parameters, the area-weighted mean crystallite size, $\langle x \rangle_{area}$, and the dislocation density, ρ, can be determined [9].

Results and Discussion

The area-weighted mean crystallite size ($\langle x \rangle_{area}$) and the dislocation density (ρ) for Al are shown as a function of true strain (ε) in Fig. 1. Experimental resuls show that the crystallite size decreased, while the dislocation density increased with increasing strain and they both saturated after 1 ECAP pass (ε~1). The minimum value of the crystallite size and the maximum of the dislocation density are 272 nm and 1.8×10^{14} m^{-2}, respectively. In the case of Al3Mg alloy, although the microstructure developed in a similar manner the saturation values of the crystallite size and the dislocation density were lower (65 nm) and higher (23×10^{14} m^{-2}), respectively, than those for pure Al. Morover, for Al3Mg, while the crystallite size saturates even after 1 pass, the saturation of the dislocation density was only obtained later, after 4 passes.

The effect of Mg solute atoms on the evolution of microstructure in Al during deformation is shown in Fig. 2 where both the crystallite size and the dislocation density after 8 ECAP passes are plotted as a function of Mg content. It can be seen that severe plastic deformation is more effective in grain refinement and in increasing the dislocation density if the Mg content is higher. These results can be explained by the effect of Mg solute atoms on the dislocation mobility. The Mg solute atoms impede the motion of dislocations in the Al matrix, hindering the annihilation of dislocations during deformation and then leading to an increase in the dislocation density. The reduced recovery rate is also the reason why the saturation of dislocation density is achieved at a higher strain for Al alloys. As grain refinement in SPD metals occurs by the arrangement of dislocations into cell boundaries, the higher dislocation density results in a decrease of crystallite size for higher Mg concentrations.

It is established that the yield strength of f.c.c. metals can be correlated either to the grain (crystallite) size or the dislocation density. In the former case the Hall-Petch equation is applied [10] while in the latter case the Taylor formula is used [2,11-13]. The grain size of SPD materials determined by transmission electron microscopy (TEM) is generally several times higher than the crystallite size (or coherently scattering domain size) obtained by X-ray line profile analysis. The reason for this difference originates from the hierarchy of the microstructure of SPD metals. The grains confined by high-angle boundaries are subdivided into subgrains and/or cells. The misorientation angle between cells is low (1-2°) therefore there is no measurable contrast difference between them in TEM micrographs and they can be observed separately only by high-resolution TEM investigations. At the same time there is no coherency between the X-rays scattered from the different cells, therefore X-ray line profile analysis measures the size of these objects. Consequently, the application of the Hall-Petch equation is rather uncertain since the substitution into the equation of either the grain size or the crystallite size determined by TEM or X-rays, respectively, may give different yield strength values.
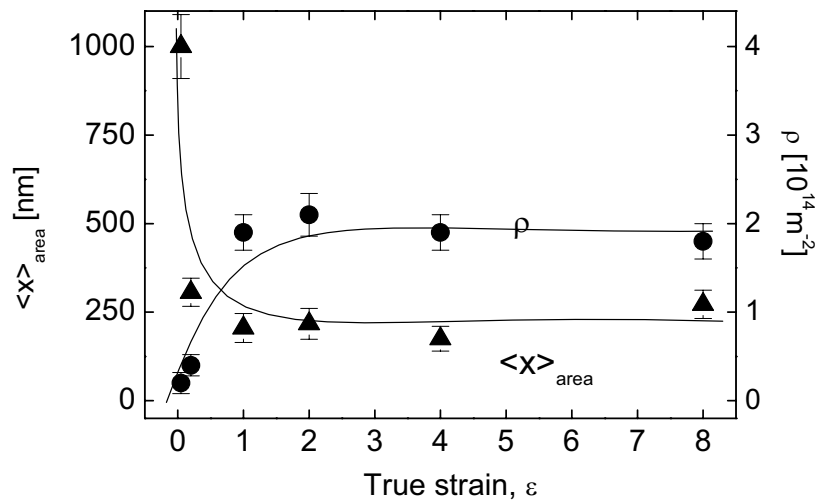

Fig. 1: The area-weighted mean crystallite size ($\langle x \rangle_{area}$) and the dislocation density (ρ) for Al as a function of the imposed strain.
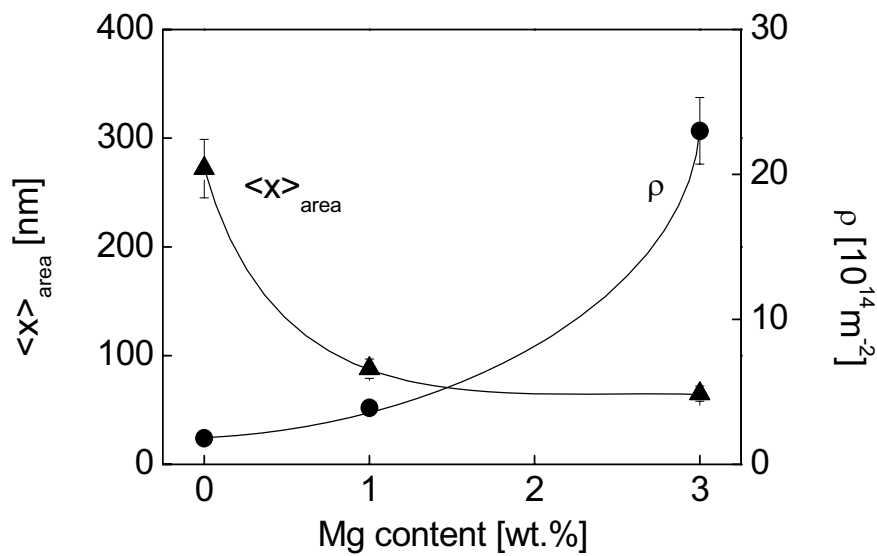

Fig. 2: The crystallite size and the dislocation density as a function of Mg content after 8 ECAP passes.

In order to examine the mechanism of the strengthening process, the yield strength obtained by mechanical tests is compared with the values calculated from the total dislocation density using the Taylor equation:

$$\sigma_{Taylor}=\sigma_0+\alpha MGb\rho^{1/2}, \qquad (1)$$

where σ is the yield strength, σ_0 is the friction stress, α is a constant (α=0.33 is taken), G is the shear modulus (G=26 GPa is taken for Al and its alloys), b is the length of the Burgers vector of dislocations (b=0.286 nm) and M is the Taylor factor (M=3 for untextured polycrystalline materials). The values of friction stress are taken as 20, 25 and 50 MPa for Al, Al1Mg and Al3Mg, respectively. The yield strength measured by mechanical tests ($\sigma_{measured}$) versus the values calculated from the Taylor equation (σ_{Taylor}) are plotted in Fig. 3. This figure also shows the data determined previously on other f.c.c. specimens, namely on pure Cu and Ni samples for which the values of $\sigma_{measured}$ are determined by tensile test and Vickers hardness measurements, respectively [14-17]. For Cu, G=42 GPa, σ_0=20 MPa and b=0.256 nm are taken in the calculation of σ_{Taylor}. For Ni, G=82 GPa, σ_0=20 MPa and b=0.249 nm are used. The Cu and Ni samples were processed as follows.

Technical purity copper specimens were processed by ECAP for 1 and 8 passes using a 90° die following route C (in which the billet is rotated by 180° around its longitudinal axis after each pass) and by compression for ε=0.7 using an MTS hydraulic machine [14,15]. High purity nickel (99.99%) was deformed by different methods of SPD, namely ECAP, high-pressure torsion (HPT) and their combinations [16,17]. Nickel cylinders having diameters of 16 mm and lengths of ~100 mm were subjected to ECAP at room temperature using a die with an internal angle of 90°. Samples were pressed repetitively for 8 passes following route B_C. For processing by HPT, disks with diameters of 10 mm and thickness of ~0.3 mm were torsionally-strained under a high pressure of 6 GPa for a total of 5 complete revolutions, equivalent to a true strain ~6. An additional sample was prepared by a combination of ECAP and HPT (designated as 8ECAP + 5HPT).
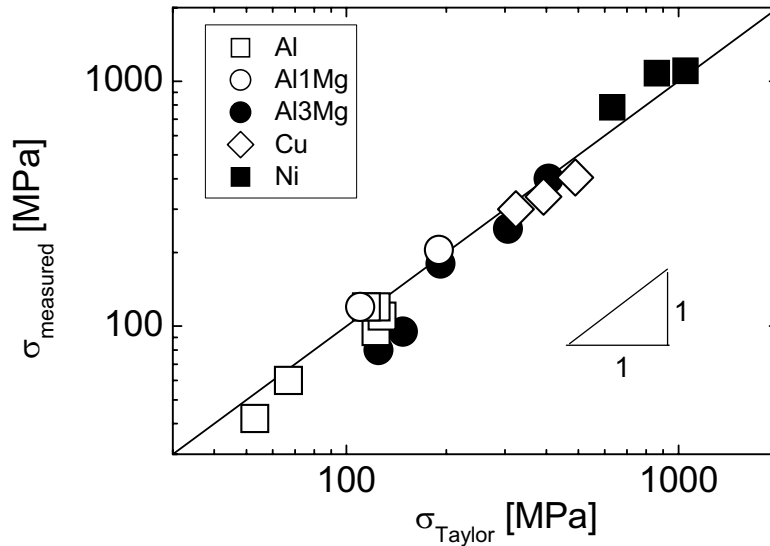

Figure 3: The yield strength measured by mechanical tests ($\sigma_{measured}$) versus the values calculated from the dislocation density according to Eq. 1 (σ_{Taylor}).

For the identification of the data points in Fig. 3, the values of the corresponding quantities are listed in Table 1. As the yield strength values span a relatively wide range, the plot in Fig. 3 is shown in double logarithmic scales for a better visualisation of the datum points at low values. It can be seen that the yield strength measured by mechanical tests are in relatively good agreement with the values calculated according to the Taylor equation (Eq. 1). The good agreement indicates that in f.c.c. metals processed by SPD the strength is basically determined by the interaction between dislocations.

During the SPD process, the dislocations formed in the grain interiors re-arrange into cell boundaries to minimise their strain-energy [2,13,18]. These objects have low-angle grain boundary character as they separate cells with small misorientations. As the deformation proceeds, the dislocation density in the cell boundaries increases (even up to 10^{17}-10^{18} m^{-2}), so that the thickness of the boundaries decreases and the misorientations between the neighboring cells also increase so that the cell boundaries are transformed into high-angle grain boundaries [2,13,19]. At a certain strain the microstructure contains low-angle cell boundaries (or incidental dislocation boundaries, IDBs) and high-angle grain boundaries (geometrically necessary boundaries, GNBs) simultaneously [13]. In these materials, two strengthening contributions should be considered: (i) dislocation strengthening due to the presence of low-angle boundaries (IDBs) and (ii) grain boundary strengthening due to medium to high-angle boundaries (GNBs). Hughes and Hansen [13] have shown theoretically that each of the two contributions can be described by a Taylor-type equation as the boundaries are built up from dislocations and.the strengthening is caused by dislocation-dislocation interactions. This is in good agreement with these experimental results. It should be noted, however, that the strengthening of GNBs can be also expressed by a Hall-Petch relationship in which the strength is determined by the average spacing between GNBs [13].

Table 1. The yield strength ($\sigma_{measured}$) and the dislocation density (ρ) data used in Fig. 3.

Al			Al1Mg			Al3Mg		
sample	$\sigma_{measured}$ [MPa]	ρ [10^{14} m^{-2}]	sample	$\sigma_{measured}$ [MPa]	ρ [10^{14} m^{-2}]	sample	$\sigma_{measured}$ [MPa]	ρ [10^{14} m^{-2}]
$\varepsilon=0.05$	42	0.2	$\varepsilon=0.2$	120	0.9	$\varepsilon=0.02$	80	1.0
$\varepsilon=0.2$	60	0.4	8ECAP	220	3.9	$\varepsilon=0.05$	95	1.7
1ECAP	95	1.9				$\varepsilon=0.2$	180	3.6
2ECAP	110	2.1				1ECAP	250	12
4ECAP	120	1.9				8ECAP	400	23
8ECAP	120	1.8						

Cu			Ni		
sample	$\sigma_{measured}$ [MPa]	ρ [10^{14} m^{-2}]	sample	$\sigma_{measured}$ [MPa]	ρ [10^{14} m^{-2}]
$\varepsilon=0.7$	300	8	8ECAP	783	9
1ECAP	338	12	5HPT	1097	17
8ECAP	405	19	8ECAP + 5HPT	1103	25

235

Summary and Conclusions

1. The evolution of microstructure in f.c.c. metals processed by ECAP was studied by X-ray line profile analysis. It was found that the crystallite size decreased and the dislocation density increased with increasing strain and their values saturated after several ECAP passses.

2. The Mg addition hinders the annihilation of dislocations in the Al matrix during deformation leading to a stronger increase and decrease of the dislocation density and the crystallite size, respectively, in ECAP Al-Mg samples. Furthermore, as a result of the Mg addition, the dislocation density saturates at a higher strain for Al-Mg alloys than for pure Al.

3. The yield strength of different f.c.c. metals produced by SPD methods is successfully described by the Taylor equation using the dislocation density values determined by X-ray line profile analysis. The most probable explanation of this result is that the obstacles of dislocation motion in SPD materials, the cell or subgrain boundaries, consist of dislocations and consequently the main strengthening mechanism is the interaction between dislocations.

References

1. R.Z. Valiev, R.K. Islamgaliev, I.V. Alexandrov, Prog. Mater. Sci. 45 (2000) 103.
2. F. Dalla Torre, R. Lapovok, J. Sandlin, P.F. Thomson, C.H.J. Davies, E.V. Pereloma, Acta Mater. 52 (2004) 4819.
3. T. Ungár, A. Borbély, Appl. Phys. Lett. 69 (1996) 3173.
4. R. Kuzel, Z. Matej, V. Cherkaska, J. Pesicka, J. Cízek, I. Procházka, R. K. Islamgaliev, J. Alloys Compd. 378 (2004) 242.
5. N. Q. Chinh, Gy. Horváth, Z. Horita, T. G. Langdon, Acta Mater. 52 (2004) 3555.
6. J. Gubicza, N. Q. Chinh, Z. Horita, T. G. Langdon, Mater. Sci. Eng. A 387-389 (2004) 55.
7. M. Furukawa, Y. Iwahashi, Z. Horita, M. Nemoto, T.G. Langdon, Mater. Sci. Eng. A 257 (1998) 328.
8. Y. Iwahashi, J. Wang, Z. Horita, M. Nemoto, T.G. Langdon, Scripta Mater. 35 (1996) 143.
9. T. Ungár, J. Gubicza, G. Ribárik, A. Borbély, J. Appl. Cryst. 34 (2001) 298.
10. A. Dubravina, M. J. Zehetbauer, E. Schafler, I. V. Alexandrov, Mater. Sci. Eng. A 387-389 (2004) 817.
11. M. J. Zehetbauer, J. Kohout, E. Schafler, F. Sachslehner, A. Dubravina, J. Alloys Compd. 378 (2004) 32.
12. E. Artz, Acta Mater. 46 (1998) 5611.
13. D. A. Hughes, N. Hansen, Acta Mater. 48 (2000) 2985.
14. J. Gubicza, N. H. Nam, L. Balogh, R. J. Hellmig, V. V. Stolyarov, Y. Estrin, T. Ungár, J. Alloys Compd. 378 (2004) 248.
15. S.C. Baik, R.J. Hellmig, Y. Estrin, H.S. Kim, Z. Metallkd. 94 (2003) 754.
16. A.P. Zhilyaev, J.Gubicza, G. Nurislamova, Á.Révész, S. Suriñach, M.D. Baró, T. Ungár, Phys. Stat. Sol. (a) 198 (2003) 263.
17. A.P. Zhilyaev, B.-K. Kim, J.A. Szpunar, M.D. Baró, T.G. Langdon, Mater. Sci. Eng. A 391 (2005) 377.
18. D.A. Hughes, Acta Metall. Mater. 41 (1993) 1421.
19. S.V. Bobylev, M. Yu. Gutkin, I.A. Ovid'ko, Acta Mater. 52 (2004) 3793.